A tumor mRNA-triggered photodynamic molecular beacon based on oligonucleotide hairpin control of singlet oxygen production†

Juan Chen,[a,d] Jonathan F. Lovell,[b] Pui-Chi Lo,[c] Klara Stefflova,[e] Mark Niedre,[c] Brian C. Wilson[a,c] and Gang Zheng*[a,b,c,d]

Received 15th January 2008, Accepted 29th May 2008
First published as an Advance Article on the web 9th June 2008
DOI: 10.1039/b800653a

We report a new class of photodynamic molecular beacon (PMB) with tumor specific mRNA-triggered control of singlet oxygen ($^1O_2$) production. The beacon contains a single-stranded oligonucleotide linker that forms a stem-loop structure (hairpin) in which the sequence is an antisense oligonucleotide (AS-ON) complementary to a target mRNA. The stem is formed by the annealing of two complementary arm sequences that are on either side of the loop sequence. A photosensitizer molecule (PS) is attached to the end of one arm and a quencher (Q) is similarly attached to the other end. The conformationally-restricted hairpin forces Q to efficiently silence the photoreactivity of PS. In the presence of target mRNA, the hairpin opens and the PS is no longer silenced. Upon irradiating with light, the PS then emits fluorescence and generates cytotoxic $^1O_2$. To show proof of concept, we have synthesized a *c-raf-1* mRNA-triggered PMB using pyropheophorbide (Pyro) as PS, carotenoid as Q and *c-raf-1* mRNA-targeted AS-ON as the loop sequence. We show that the $^1O_2$ production of Pyro is quenched in its native state by 15-fold and is restored 9-fold by the addition of the target RNA. Comparing this to our recently reported self-folding peptide linker-based PMB, the hairpin effect results in an enhanced $^1O_2$ quenching efficiency that decreases the residual $^1O_2$ production by over 3-fold, thus providing enhanced control of $^1O_2$ production upon target-linker interactions. When incubated with *c-raf-1* expressing MDA-MB-231 cancer cells, the PMB displayed efficient cellular uptake and subsequently effective PDT activation in targeted cells.

Introduction

Photodynamic therapy (PDT) is an approved cancer therapy relying on *in situ* generation of cytotoxic singlet oxygen ($^1O_2$) by activation of a photosensitizer (PS) with light.[1] By controlling how the light and the PS are delivered to tumor tissues, some degree of PDT selectivity can be achieved. We recently introduced a novel photodynamic molecular beacon (PMB) concept for controlling the ability of the PS to generate $^1O_2$, providing an additional degree of selectivity.[2–5] This PMB consisted of a peptide linker that is sequence specific to a cancer-associated protease. A PS and a $^1O_2$ quencher (Q) were conjugated to the opposite ends of the linker. Proximity of the PS and Q can efficiently inhibit $^1O_2$ generation through energy transfer. In the presence of a specific protease, the substrate sequence is cleaved and the PS and Q separate, so that the PS can then be photo-activated. Thus, the ability of a PS to generate $^1O_2$ can be switched on, depending on specific linker–target interactions. This enables the beacons to achieve a very high PDT selectivity by destroying only the targeted cancer cells (through $^1O_2$ generation), leaving non-targeted cells unharmed. This $^1O_2$ quenching/activation paradigm was initially demonstrated using a peptide-based caspase 3-triggered PMB,[2] and has been validated in cancer cells *in vitro* and *in vivo* using a matrix metalloproteinase-7 (MMP7) trigger.[3]

The main advantage of the protease-triggered PMB is that the PDT efficacy is no longer dependent only on how the PS is delivered to the cancer cells. Rather, it will depend also on how specific this protease is to be expressed in the cancer cells and how selective the PMB is to this protease. Perhaps more importantly, the PDT efficacy will also depend on how completely the photoreactivity of the PS is silenced in the quenched state, since any residual $^1O_2$ production in non-targeted cells could lead to phototoxicity to healthy tissues. From this perspective, the approach to date has been limited by two factors: (1) the total dependence of the $^1O_2$ quenching on the random folding of the peptide linker before protease cleavage, which could also be microenvironment-dependent, and (2) the limited specificity of protease target expression in tumor *versus* normal tissues. Hence, choosing biomarkers with higher tumor specificity and achieving higher specific quenching/activation mechanisms are two directions to further improve the PMB's selectivity.

Many cancers are characterized by abnormal gene expression. Thus, using antisense oligonucleotide (AS-ON) and short interfering RNA (siRNA) molecules to disrupt these aberrantly

[a]*Division of Biophysics and Bioimaging, Ontario Cancer Institute, Toronto, Ontario, M5G 1L7, Canada. E-mail: gang.zheng@uhnres.utoronto.ca; Fax: +1-416-581-7666; Tel: +1-416-581-7666*
[b]*Institute of Biomaterials and Biomedical Engineering, Toronto, Ontario, M5G 1L7, Canada*
[c]*Department of Medical Biophysics, University of Toronto, Toronto, Ontario, M5G 1L7, Canada*
[d]*Department of Radiology, University of Pennsylvania, Philadelphia, Pennsylvania, 19104, USA*
[e]*Department of Chemistry, University of Pennsylvania, Philadelphia, Pennsylvania, 19104, USA*
† Electronic supplementary information (ESI) available: Additional experimental data. See DOI: 10.1039/b800653a

expressed genes at the level of mRNA transcription has evolved rapidly over the past few years.[6–8] The high tumor specificity of these mRNAs, plus the fact that their hybridization to the complementary AS-ON sequences by means of Watson–Crick base pairing is a highly selective and efficient process, make them attractive targets for a new class of PMBs. In a recent study, Clo *et al.* introduced the nucleic acid-based $^1O_2$ control principle.[9] In their approach, a PS and a Q were respectively attached to two single DNA strands which complement each other. They have confirmed that the hybridization of these two DNA strands can bring the PS and the Q into close proximity that generates effective $^1O_2$ quenching. Upon competitive hybridization with a nucleic acid target, $^1O_2$ production was switched on. Here, we are interested in constructing a PS and a Q in a single molecule by taking advantages of the original hairpin-based molecular beacon principle.[10] The hairpin beacons commonly feature a stem-loop oligonucleotide that brings a quencher close to a fluorophore to silence its fluorescence. Once the loop sequence of the hairpin hybridizes with target complementary nucleic acid, it unfolds to restore the fluorescence. These beacons can offer precise fluorescence emission control because of their high level of fluorescence quenching in the native state, due to the hairpin conformation.

By the combination of this classic hairpin beacon design with our PMB principle, we report here a new class of nucleic acid-triggered PMBs for the selective control of $^1O_2$ generation. As depicted in Fig. 1, this mRNA-PMB consists of a single-stranded oligonucleotide attaching the PS and Q on the opposite ends of a hairpin structure, such that $^1O_2$ generation is quenched until hybridization of the antisense oligonucleotide (AS-ON) loop with tumor-specific mRNA. We expected this novel PMB would be able to greatly enhance the control of $^1O_2$ production, since (1) the confined geometry and fixed distance between PS and Q *via* the hairpin structure should maximize the $^1O_2$ quenching, (2) the high fidelity of nucleic acid hybridization should improve the specificity for target-linker interactions, (3) the expression profile of an mRNA target could have a higher tumor *versus* normal tissue ratio than that of proteases, and (4) the development of modern RNA-based therapeutics (*e.g.*, siRNA) could offer a unique opportunity for synergistic therapeutic effects with PDT. In this paper, we will describe the synthesis and characterization of an mRNA-PMB and the evaluation of its fluorescence and $^1O_2$ control in solution. We also report preliminary observations showing that this PMB is self-delivered into intact cancer cells without the aid of transfection agents and that it is toxic to the targeted cells upon irradiation with light.

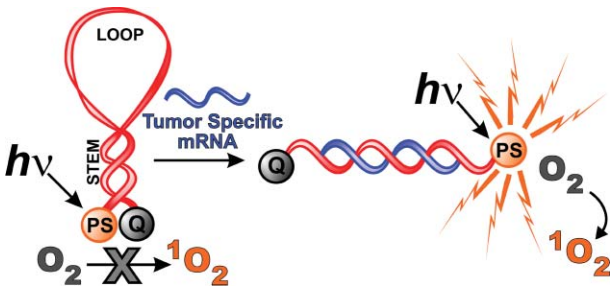

Fig. 1 The concept of mRNA-triggered PMBs.

Results

Design and synthesis of *c-raf-1* mRNA targeted PMB

For proof-of-concept, we designed the first prototype mRNA-PMB using *c-raf*-1 mRNA as the trigger, which is a well known antisense therapeutic target due to its role in the activation of MAP kinase pathways and malignant transformation.[11] The rationale and strategy for this particular *c-raf-1* mRNA targeted PMB were as follows: (1) *Choice of backbone*: A 2′-O-methyl RNA backbone was selected because of its high affinity for RNA, faster hybridization, high nuclease resistance and good stability against RNase H digestion upon hybridization.[12] (2) *Choice of PS and Q*: Pyropheophorbide (Pyro) and carotenoid (CAR) were chosen as PS and Q, respectively, based on previous studies demonstrating this is a functional pair for $^1O_2$ quenching/activation.[2] (3) *Hairpin sequence*: In order to find a sequence that is easily accessible to target mRNAs, the *c-raf-1* mRNA-targeting AS-ON drug (ISIS 5132)[11] was adapted into the 2′-O-methyl RNA backbone, UCCCGCCUGUGACAUGCAUU, as the loop sequence. Finally, 5-mer stem sequences were used to optimize the balance between the rate of target hybridization and the hybridization specificity.[13] The synthetic protocol of this *c-raf-1* mRNA-triggered PMB, CAR-5′GCGAGUCCCGCCUGUGACAUGCAUUCUCGC-3′-Pyro (P30C, stem underlined), is depicted in Fig. 2. Following this protocol, P30C was successfully synthesized and purified by HPLC. Its structure and purity were confirmed by its HPLC chromatogram (Fig. 3A showing P30C retention time = 35 min), UV-Vis spectrum (Fig. 3B showing the specific absorbance peaks corresponding to Pyro at 414 and 664 nm, CAR at 472 and 501 nm and oligonucleotide at 260 nm) and MALDI-ToF spectrum (Fig. 3C showing the molecular weight: calc. 11327.8, found 11326.3). A positive control, 5′-GCGAGUCCCGCCUGUGACAUGCAUUCUCGC-3′-Pyro (P30, without quencher moiety), and a random sequence control, 5′CARGCGAGACCGCCGCAUUUGAUCGAUACUCGC-3′-Pyro (r-P30C), were also synthesized and characterized by their mass spectra (molecular weight for P30: calc. 10632.64, ESI-MS found 10633.5; molecular weight for r-P30C: calc. 11374.8, MALDI-ToF found 11373.8).

Validation of the specific interactions of target-beacon

To evaluate the photoreactivity of P30C, the fluorescence of P30C was compared with the no-quencher positive control, P30, at the same concentration. P30C produced 16-fold less fluorescence than P30, indicating that the oligonucleotide linker hairpin conformation resulted in very efficient quenching of Pyro by CAR. To test the P30C activation upon hybridization with the target RNA, its fluorescence was measured in the presence of a target RNA and a 1-basepair mismatched RNA. A similar study was also performed on the scrambled control, r-P30C, comprising P30C with a random-loop sequence. As shown in Fig. 4, P30C produced a 13-fold fluorescence increase upon hybridization with the target RNA but only a 3-fold increase with 1-basepair mismatched RNA, while r-P30C showed no measurable increase with the target RNA. Hence, the hairpin PMB can distinguish target mRNA sequences at a single-base level, which is consistent with classic molecular beacons.[10,14–17]

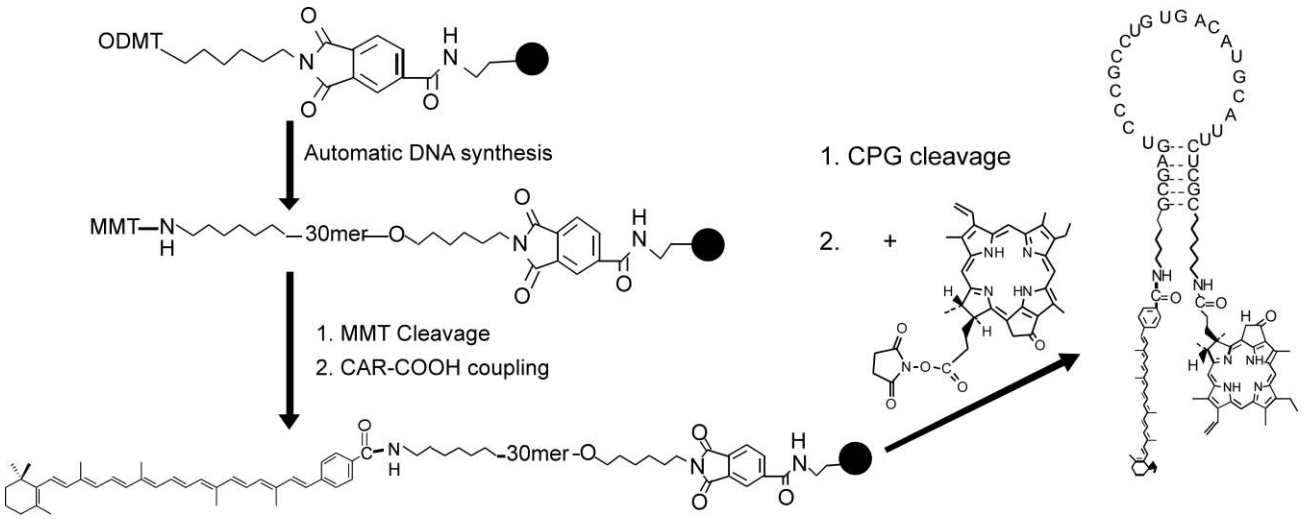

Fig. 2 The synthesis of *c-raf-1* mRNA-triggered PMB (P30C).

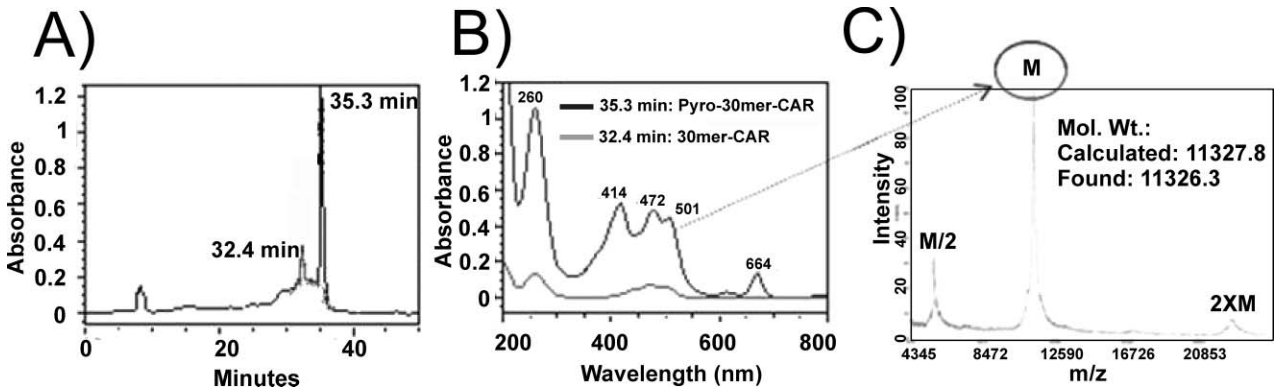

Fig. 3 The characterization of P30C: (A) the HPLC chromatograph; (B) the corresponding UV-vis spectra and (C) the MALDI-ToF mass spectrum.

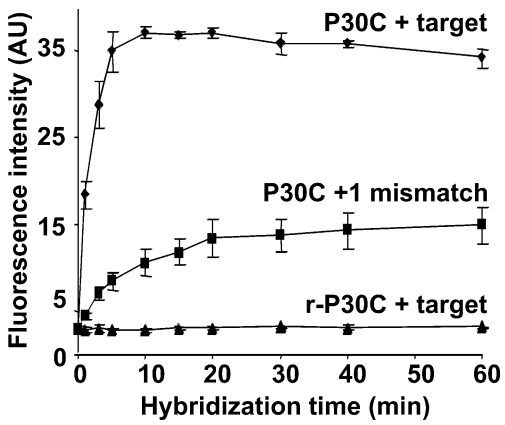

Fig. 4 Fluorescence activation as a function of hybridization time in solution, comparing fluorescence activation of (1) P30C with target, (2) P30C with 1-basepair mismatched target and (3) scrambled beacon r-P30C with target.

Validation of the $^1O_2$ quenching and activation

To determine the role of the hairpin-based oligonucleotide linker in controlling the ability of PS to generate $^1O_2$, the $^1O_2$ near-infrared (NIR) (1270 nm) luminescence of P30, P30C, P30 + target RNA and P30C + target RNA were measured. P30 was used as a positive control to quantify the ability of Pyro to produce $^1O_2$ and all experimental samples were prepared at the same molar concentration of Pyro. As shown in Fig. 5, P30C produced 93% less $^1O_2$ luminescence than P30. This quenching efficiency is much higher than that was observed in our previous reported peptide linker-based PMB with the same PS/Q pair (78% quenching efficiency observed for Pyro-GDEVGGSGK-CAR, PPC).[4] These data suggest that the hairpin-restricted oligonucleotide linker can force Q to more efficiently silence the PS's photodynamic function than the self-folding peptide linker. As a result, over 3-fold decrease of residual $^1O_2$ production in P30C (6.7%) compared to PPC (22%) will offer an improved photoprotective effect in non-targeted cells to minimize their photodamage.

To determine if the $^1O_2$ activation of P30C is also sequence-specific to target RNAs, two equivalents of complementary target RNA sequences were added to the solution of P30 and P30C. As shown in Fig. 5, the addition of the target resulted in a 9-fold $^1O_2$ increase in P30C after 30 min incubation, whereas it had no measurable effect with P30. Moreover, the degree of $^1O_2$ restoration in P30C + target (induced by target-loop hybridization) was 63%, similar to the 67.5% found in PPC + caspase-3 (a previous peptide-based beacon activated by proteolytic cleavage of the peptide linker),[4] suggesting that the hairpin-disassociation induced PS

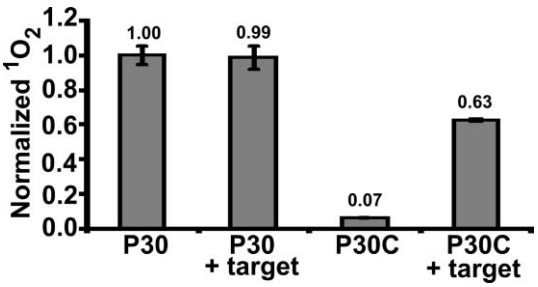

Fig. 5 $^1O_2$ production and activation of the hairpin-based mRNA triggered beacon (P30C) was measured in solution directly by near-infrared luminescence.

activation is almost equally effective as the linker-cleavage induced PS activation. As we have noted previously in proteolytic cleavage triggered PMBs,[4] the greater than 30% unrestored $^1O_2$ production in P30C + target RNA is likely due to the photoprotective role of CAR in directly scavenging $^1O_2$. This could result in some loss of PDT potency of P30C toward targeted cells. However, as a "trade off", the scavenger role of CAR could also lead to a very high level of "protection" for non-targeted cells. On the other hand, it may be desirable in the future to use quenchers that do not scavenge $^1O_2$ to bypass this problem.

Taken together, these results clearly demonstrate that $^1O_2$ production (and fluorescence emission) of P30C is activated specifically in response to the target RNA sequence.

Intracellular uptake of P30C

To test the intracellular uptake of P30C, confocal fluorescence imaging was preformed on MDA-MB-231 cells, a human breast epithelial adenocarcinoma cell line over-expressing *c-raf-1* mRNA.[11] Oligonucleotides are extremely charged and normally cannot be delivered to cells without special reagents and protocols. Unexpectedly, P30C displayed remarkably efficient cellular uptake without the aid of transfection agents. As shown in Fig. 6A–C, MDA-MB-231 tumor cells incubated for 4 h with 50 μM of P30C (or P30 as a positive control) showed significant intracellular fluorescence (extra nuclear), compared with the unincubated cells. This not only confirmed the P30C activation in *c-raf-1* mRNA over-expressing cells but also suggests a previously unknown Pyro (non-cationic porphyrin)-driven oligonucleotide delivery mechanism. To clarify this finding, a classic molecular beacon, F30B, was synthesized using the same hairpin linker but with fluorescein (FAM) and black hole quencher 1 (BHQ1) as the fluorophore/quencher pair. Due to perfect spectral overlap, BHQ1 should efficiently quench the FAM fluorescence but not $^1O_2$. As shown in Fig. 6D–F, cells incubated with 50 μM of either F30B or F30 (without BHQ1) showed no fluorescence, whereas cells co-incubated with 50 μM of F30B and 0.05 g L^{-1} of Lipofectamine™ 2000 (Invitrogen, Carlsbad, CA, USA) showed strong intracellular fluorescence. This suggests that it is the Pyro component in P30C that is responsible for the efficient delivery of the beacon into cancer cells. Studies of the possible mechanisms of this intracellular delivery are ongoing.

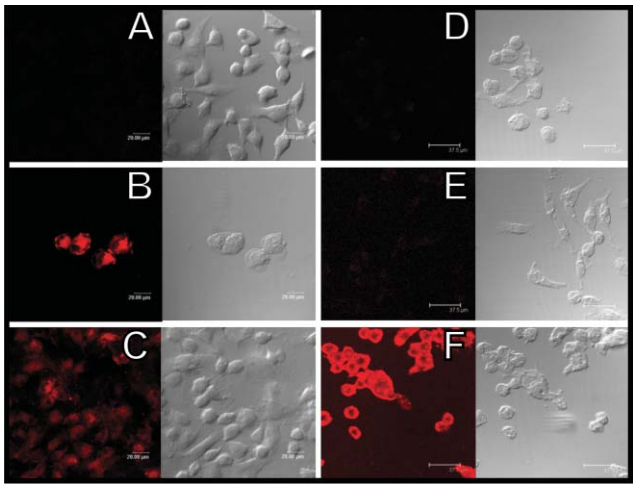

Fig. 6 Confocal images of MDA-MB-231 cells: cells alone (A), cells incubated with (B) 50 μM of P30, (C) 50 μM of P30C, (D) 50 μM of F30, (E) 50 μM of F30B and (F) co-incubated with 50 μM of F30B and 0.05 g L^{-1} of Lipofectamine™ 2000 for 4 h.

In vitro PDT efficacy of P30C

To test the PDT efficacy of P30C in targeted cells, the cell viability of MDA-MB-231 cells treated with P30C, P30 (positive control) or r-P30C (negative control) were measured before and after light treatment. Cell viability was normalized to the control cells (no drug or light). The results are shown in Fig. 7. The viability of cells incubated with 2 μM of P30C, P30 or r-P30C without light treatment did not show significant cell toxicity compared with that of the control cells without drug and light, indicating minimal dark toxicity under these incubation conditions. Upon PDT treatment, both P30 and P30C showed light dose-dependent PDT response. With 5 J cm^{-2} of light exposure, 2 μM of P30C reduced the viability to 38.0 ± 5.8%, which is similar to that of 2 μM positive control P30 (31.1 ± 6.6%) ($p < 0.05$). The fact that P30C and P30 have almost identical PDT responses *in vitro* suggests that the photoactivity of P30C can be fully restored in cells expressing the target c-raf-1 mRNA. More importantly, after 5 J cm^{-2} of light exposure, the scrambled beacon r-P30C showed significantly less PDT efficacy (81.0 ± 4.6%) when compared with both P30 (31.1 ± 6.6%) and P30C (38.0 ± 5.8%) at the same concentration ($p < 0.05$). No significant difference was observed between r-P30C

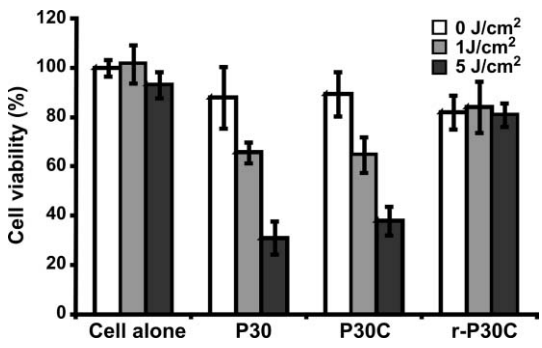

Fig. 7 Photodynamic cytotoxicity determined by cell viability (MTT) assay. Viability of MDA-MB-231 cells after incubated with 2 μM of P30, P30C or r-P30C and treated with different PDT light doses (1, 5 J cm^{-2}) compared with cell alone that serve as the 100% viable reference. Means ± standard deviation for triplicate experiments.

with or without light treatment (81.0 ± 4.6% *versus* 82.0 ± 6.9%) ($p < 0.05$). These preliminary data suggested that photoactivation of P30C is triggered by c-raf-1 mRNA.

Discussion

Hairpin-based molecular beacons allow the fluorometric identification of target nucleic acids with great specificity.[10] Due to the importance of understanding gene expression, they have seen considerable interest and investigation and they are the best tool to facilitate mRNA detection in live cells.[13,14,17–26] In this work, we showed proof of principle for an entirely new use for these classic molecular beacons—discriminate cell killing based on specific mRNA expression. This mRNA-triggered PMB approach combines the specificity of molecular beacons with the light induced toxicity of photodynamic therapy.

Our hairpin mRNA-PMB displayed good specificity to *c-raf-1* mRNA. While *c-raf*-1 is an important cancer gene, it should be noted that there are probably better targets than *c-raf*-1 since this gene is widely expressed in both cancer and non-cancer tissues. Addition of the target mRNA resulted in a 13-fold increase in fluorescence, while scrambled beacon was unresponsive to the target mRNA. This PMB can also distinguish target mRNA sequences at a single-base level, which is consistent with classic molecular beacons. The increase of singlet oxygen production in the beacon over the background level will be one of the most important metrics of successful cell killing in response to target mRNA. We suspect that the hybridized PMB generates enough $^1O_2$ upon irradiation to induce an apoptotic response in the cells, although it is unclear exactly how the cells are killed and whether or not the PMB is stable during that period. The 9-fold increase in singlet oxygen production achieved with the PMB is in line with the 10-fold fluorescence increases reported for many conventional molecular beacons,[16,17] although others have observed larger increases of up to 60-fold.[14] Compared to our previous self-folding peptide linker-based PMBs,[4] this hairpin oligonucleotide based PMB displayed a more than 3-fold greater signal-to-noise ratio. This suggests that nucleic acid PMBs will inflict minimal harm to cells that do not express the target RNA when irradiated with light.

Optimal activation of the PMB is dependent on both amount of target mRNA molecules and PMBs in cells. If there are too few copies of the target mRNA, PMBs may not be activated efficiently. If there are too few copies of the PMB, the signal generated may be too low. To estimate the number of copies of target *c-raf*-1 in MDA-MB-231 cells, a previously reported quantitative polymerase chain reaction (qPCR) technique[27] was used. Based on the qPCR result, a similar level of *c-raf*-1 expression relative to the reference TATA box binding protein (TBP) (see electronic supplementary information, ESI) was detected, suggesting there were approximately 1000 of *c-raf*-1 mRNA transcripts per cell. However, the signal generated by the PMBs in cells may come from more than 1000 activated PMBs, since upon binding to their target, the PMB-target complex may remain stable, while more *c-raf*-1 transcripts continue to be generated and bind additional PMBs. Therefore, MDA-MB-231 cell is a suitable cell line to test the *c-raf-1*-PMB activation.

The delivery of the nucleic acid-based PMBs to cancer cells is a further challenge for *in vitro* and *in vivo* validation and any potential clinical applications. Nucleic acids are predominantly negatively charged, making it difficult for them to diffuse passively across the cell membrane. Many methods, ranging from mechanical approaches like microinjection[28] and electroporation,[29] to chemical approaches like neutralizing the charge by forming complexes with cationic compounds (cationic liposomes,[30] porphyrins,[31] peptides[23,32–34] *etc.*), to biological approaches like using viral vectors, have all been tested.[35,36] However, successful and safe *in vivo* nucleic acid delivery strategies remain elusive. This makes the finding that P30C can be self-delivered to human breast cancer cells surprising and potentially significant. Although the mechanism of the uptake is not clearly known, cationic porphyrins have been used previously as oligonucleotide transfection agents,[31] even though that technique did not involve covalent attachment.

Conclusion

We have developed a novel mRNA-PMB strategy by attaching a PS and a Q at each end of a hairpin-based oligonucleotide linker to achieve cell killing based on specific mRNA expression. We have confirmed that the hairpin effect accounts for a higher quenching efficiency that results in a more than 3-fold greater signal to noise ratio when compared with self-folding peptide linker-based PMB, thus providing enhanced control of $^1O_2$ production upon target-linker interactions. The mRNA-PMB displays a good self-driven cellular uptake and subsequently effective PDT activation in targeted cells. Given the increasing knowledge of genetic biomarkers of cancers (and other diseases), the mRNA-PMB strategy has potential to generate a wide range of clinically useful PDT agents with high selectivity due to the specificity of the nucleic acid hybridization process, the highly efficient hairpin-based $^1O_2$ quenching, the growing number of known tumor-specific mRNAs and the rapid development of RNA therapeutics (*e.g.*, siRNAs).

Experimental

UV-Vis and fluorescence spectra were recorded on a Perkin-Elmer (Boston, MA, USA) Lambda 20 spectrophotometer and a LS-50B spectrofluorometer, respectively. MALDI-ToF MS spectra were measured by an Applied Biosystems (Foster City, CA, USA) Voyager System 2070. Reverse phase (RP) analytical HPLC was performed on Zorbex RP-C8 (4.6 mm × 250 mm) column using a Waters (Milford, MA, USA) alliance 600 system with a Waters 2996 photodiode array and 2475 Multi λ fluorescence detectors. HPLC method: solvent A = 0.1 M TEAA buffer; solvent B = acetonitrile; gradient: from 90% of A and 10% of B to 100% of B over 45 min; flow rate: 1.0 mL min^{-1}).

Synthesis of P30C

Linker synthesis and CAR conjugation on solid phase. As shown in Fig. 2, a single-strand, 30mer 2′-OMethyl RNA sequence (GCGAGUCCCGCCUGUGACAUGCAUUCUCGC) with a 5′-C6 monomethoxytritylamino (MMT) modifier was custom synthesized on the 3′-pthalimidyl-modified CPG by the TriLink BioTechnologies (San Diego, CA). The MMT protecting group on the oligonucleotide linker (1.0 μmol) was removed by 2.5% trichloroacetic acid (TCA) in dichloromethane (DCM). The exposed free amine group was then conjugated with CAR-acid

(1.6 mg, 3 μmol) in 3 mL of *N*,*N*-dimethylformamide (DMF) with the activation reagents 1-hydroxybenzotriazole (HOBt, 0.41 mg, 3 μmol) and *O*-(benzotriazol-1-yl)-*N,N,N′,N′*-tetramethyluronium hexafluorophosphate (HBTU, 1.14 mg, 3 μmol). After shaking at room temperature under argon for 20 h, this CPG was washed with DMF and dried under high vacuum. After treated with 2 mL of concentrated ammonium hydroxide at 55 °C for 17 h, the CAR-conjugated linker oligonucleotide was cleaved from the CPG and the protecting groups of all nucleic acid bases, as well as the pthalimidyl group on its 3′ end, were removed to give the 5′-CAR-30mer-3′-NH_2. The product was then purified by HPLC.

Pyro conjugation in solution phase. Pyro-NHS (0.63 mg, 1 μmol) was conjugated to the 3′ end of the (5′-CAR-30mer-3′-NH_2) in 0.5 mL dimethylsulfoxide (DMSO) in the presence of 1% *N*,*N*-diisopropylethyl amine (DIPEA) for 4 h under argon. The crude product was purified by HPLC to give the desired 5′-CAR-30mer-3′-Pyro (P30C) with 90% yield. Following the same protocol, P30C with a random-loop sequence (ACCGCCGCAUUUGAUCGAUA), 'r-P30C', was also synthesized as a scrambled control.

Synthesis of positive control 5′-30mer-3′-Pyro (P30)

A 5′-30mer-(3′-pthalimidyl-CPG) (without 5′ end amino modification) was custom synthesized by TriLink and treated with 2 mL of concentrated ammonium hydroxide at 55 °C for 17 h. The acquired 5′-30mer-3′-NH_2 (0.2 μmol) was conjugated with Pyro-NHS (0.3 μmol) in 0.5 mL DMSO in the presence of 1% DIPEA for 4 h under argon. The crude product was purified by HPLC to give 5′-30mer-3′-Pyro (P30) as the positive control.

Target sequence synthesis

A 20mer RNA sequence, AAUGCAUGUCACAGGCGGGA, selected from wild-type *c-raf-1* mRNA, was synthesized by Dharmacon Inc (Chicago, IL USA) as the complementary target for P30C, referred to as "target RNA". In order to verify the specific interaction of P30C with the target RNA, another 20mer RNA sequence, AAUGCAUGU***A***ACAGGCGGGA, with one mismatched base (in bold italics) when compared with the target RNA, was also synthesized as the control target, referred to as "1-basepair mismatched target".

Fluorescence detection of P30C activation

P30C was dissolved in hybridization buffer (0.3 mM $MgCl_2$, 20 mM Tris–HCl, pH 8.2) to make a 0.2 μM solution. Excess target RNA or 1-basepair mismatched target (final concentration 0.4 μM) were added to the solution, respectively. The fluorescence of these solutions was monitored in real time at 37 °C at excitation/emission wavelengths 647/660 nm.

$^1O_2$ measurement assays

PDT-generated $^1O_2$ was quantified in solutions of P30, P30 + target RNA, P30C, P30C + target RNA, by measuring NIR luminescence emission at 1270 nm using an instrument and technique that have been described previously.[37] Briefly, a 10 ns pulsed 524 nm laser excited the solution. The luminescence spectrum was sampled, after rejection of background luminescence, using a set of interference filters, with a high-sensitivity NIR photomultiplier tube (H9170-45, Hamamatsu, USA) operating in time-resolved, single photon counting mode.

Cell lines

MDA-MB-231 cells were purchased from ATCC (Manassas, VA, USA). They were cultured in OPI-MEM I medium supplemented with 10% fetal bovine serum (FBS) at 37 °C in a humidified atmosphere with 100% air.

Confocal microscopy

MDA-MB-231 cells were grown for 3 days in 4-well Lab-Tek chamber slides (Naperville, IL). Experiments were started, after 3 quick washes with ice-cold PBS buffer, by addition of 200 μL of OPI-MEM I medium containing 100 μM of beacon, with or without 10 μL of Lipofectamine™ 2000. After 4 h incubation at 37 °C with 100% air, the cells were washed 5 times with ice-cold PBS buffer. The chamber slides were then mounted, sealed and imaged by confocal microscopy with 633 nm excitation and >650 nm detection.

MTT assay

MDA-MB-231 cells were grown for two days in 96-well plates. Experiments were started, after one quick wash with ice-cold PBS buffer, by addition of 100 μL of cell growth medium containing indicated amounts of P30C and control P30. After 16 h incubation at 37 °C with 100% air, the cells were washed twice with ice-cold PBS buffer and then 100 μL of cell growth medium was added. PDT treatment was performed using a 670 nm CW laser with one of two different light fluences (1 or 5 J cm^{-2}). The cells were allowed to continue growth for 24 h, at which time the MTT tracer, 3-(4,5-dimethylthiazol-2-yl)-2,5-diphenyltetrazolium bromide (ATCC, Manassas, VA, USA) was added to the medium at 0.5 mg/mL. Two hours later, the medium was removed and replaced with 150 μL of 1 : 1 DMSO: 70% isopropanol in 0.1 M HCl. The absorbance at 570 nm was measured on a Bio-tek ELx model 800 plate reader (MTX Lab System Inc., Vienna, VA, USA) to yield a measure of photodynamic cell kill.

Abbreviations

PDT, photodynamic therapy; PMB, photodynamic molecular beacon; mRNA-PMB, mRNA-triggered PMB; PS, photosensitizer; $^1O_2$, singlet oxygen; Q, $^1O_2$ quencher; CAR, carotenoid; Pyro, pyropheophorbide; P30, 30mer hairpin linker-Pyro-3′; P30C, 5′-CAR-30mer hairpin linker-Pyro-3′; MDA-MB-231, a human breast epithelial adenocarcinoma cells, over-expressing *c-raf-1* mRNAs; MTT, 3-(4,5-dimethylthiazol-2-yl)-2,5-diphenyltetrazolium bromide.

Acknowledgements

This work was supported by grants from the Canadian Cancer Society through the National Cancer Institute of Canada (#018510 to GZ and #014245 to BCW). This work was also supported by grants to GZ from US Army DAMD17-03-1-0373, NIH R21-CA95330 and the Tanenbaum/Brazilian Ball Chair in Prostate

Cancer Research. The authors would like to thank Dr Jerry Glickson, Dr Britton Chance, Dr Ponzy Lu and Dr Allen Gewirtz of the University of Pennsylvania for their support, as well as Vincent Nadeem and the James Pan lab at the Campbell Family Institute of Breast Cancer Research for assistance with qPCR.

References

1 T. J. Dougherty, C. J. Gomer, B. W. Henderson, G. Jori, D. Kessel, M. Korbelik, J. Moan and Q. Peng, Photodynamic therapy, *J. Natl. Cancer Inst.*, 1998, **90**, 889–905.

2 J. Chen, K. Stefflova, M. J. Niedre, B. C. Wilson, B. Chance, J. D. Glickson and G. Zheng, Protease-triggered photosensitizing beacon based on singlet oxygen quenching and activation, *J. Am. Chem. Soc.*, 2004, **126**, 11450–11451.

3 G. Zheng, J. Chen, K. Stefflova, M. Jarvi, H. Li and B. C. Wilson, Photodynamic molecular beacon as an activatable photosensitizer based on protease-controlled singlet oxygen quenching and activation, *Proc. Natl. Acad. Sci. USA*, 2007, **104**, 8989–8994.

4 J. Chen, M. Jarvi, P. C. Lo, K. Stefflova, B. C. Wilson and G. Zheng, Using the singlet oxygen scavenging property of carotenoid in photodynamic molecular beacons to minimize photodamage to non-targeted cells, *Photochem. Photobiol. Sci.*, 2007, **6**, 1311–1317.

5 K. Stefflova, J. Chen and G. Zheng, Killer beacons for combined cancer imaging and therapy, *Curr. Med. Chem.*, 2007, **14**, 2110–2125.

6 J. B. Opalinska and A. M. Gewirtz, Nucleic-acid therapeutics: basic principles and recent applications, *Nat. Rev. Drug Discovery*, 2002, **1**, 503–514.

7 G. R. Devi, siRNA-based approaches in cancer therapy, *Cancer Gene Ther.*, 2006, **13**, 819–829.

8 E. Iorns, C. J. Lord, N. Turner and A. Ashworth, Utilizing RNA interference to enhance cancer drug discovery, *Nat. Rev. Drug Discovery*, 2007, **6**, 556–568.

9 E. Clo, J. W. Snyder, N. V. Voigt, P. R. Ogilby and K. V. Gothelf, DNA-programmed control of photosensitized singlet oxygen production, *J. Am. Chem. Soc.*, 2006, **128**, 4200–4201.

10 S. Tyagi and F. R. Kramer, Molecular beacons: probes that fluoresce upon hybridization, *Nat. Biotechnol.*, 1996, **14**, 303–308.

11 B. P. Monia, J. F. Johnston, T. Geiger, M. Muller and D. Fabbro, Antitumor activity of a phosphorothioate antisense oligodeoxynucleotide targeted against C-raf kinase, *Nat. Med.*, 1996, **2**, 668–675.

12 A. Tsourkas, M. A. Behlke and G. Bao, Hybridization of 2′-O-methyl and 2′-deoxy molecular beacons to RNA and DNA targets, *Nucleic Acids Res.*, 2003, **31**, 5168–5174.

13 J. Perlette and W. Tan, Real-time monitoring of intracellular mRNA hybridization inside single living cells, *Anal. Chem.*, 2001, **73**, 5544–5550.

14 D. L. Sokol, X. Zhang, P. Lu and A. M. Gewirtz, Real time detection of DNA.RNA hybridization in living cells, *Proc. Natl. Acad. Sci. USA*, 1998, **95**, 11538–11543.

15 W. Tan, X. Fang, J. Li and X. Liu, Molecular beacons: a novel DNA probe for nucleic acid and protein studies, *Chemistry*, 2000, **6**, 1107–1111.

16 A. Tsourkas, M. A. Behlke, S. D. Rose and G. Bao, Hybridization kinetics and thermodynamics of molecular beacons, *Nucleic Acids Res.*, 2003, **31**, 1319–1330.

17 X. H. Peng, Z. H. Cao, J. T. Xia, G. W. Carlson, M. M. Lewis, W. C. Wood and L. Yang, Real-time detection of gene expression in cancer cells using molecular beacon imaging: new strategies for cancer research, *Cancer Res.*, 2005, **65**, 1909–1917.

18 D. P. Bratu, B. J. Cha, M. M. Mhlanga, F. R. Kramer and S. Tyagi, Visualizing the distribution and transport of mRNAs in living cells, *Proc. Natl. Acad. Sci. USA*, 2003, **100**, 13308–13313.

19 A. K. Chen, M. A. Behlke and A. Tsourkas, Avoiding false-positive signals with nuclease-vulnerable molecular beacons in single living cells, *Nucleic Acids Res.*, 2007, **35**, e105.

20 Z. Q. Cui, Z. P. Zhang, X. E. Zhang, J. K. Wen, Y. F. Zhou and W. H. Xie, Visualizing the dynamic behavior of poliovirus plus-strand RNA in living host cells, *Nucleic Acids Res.*, 2005, **33**, 3245–3252.

21 M. Kloc, K. Wilk, D. Vargas, Y. Shirato, S. Bilinski and L. D. Etkin, Potential structural role of non-coding and coding RNAs in the organization of the cytoskeleton at the vegetal cortex of Xenopus oocytes, *Development*, 2005, **132**, 3445–3457.

22 T. Matsuo, In situ visualization of messenger RNA for basic fibroblast growth factor in living cells, *Biochim. Biophys. Acta*, 1998, **1379**, 178–184.

23 N. Nitin, P. J. Santangelo, G. Kim, S. Nie and G. Bao, Peptide-linked molecular beacons for efficient delivery and rapid mRNA detection in living cells, *Nucleic Acids Res.*, 2004, **32**, e58.

24 A. J. Rodriguez, J. Condeelis, R. H. Singer and J. B. Dictenberg, Imaging mRNA movement from transcription sites to translation sites, *Semin. Cell Dev. Biol.*, 2007, **18**, 202–208.

25 A. Wang, A. M. Salazar, M. V. Yates, A. Mulchandani and W. Chen, Visualization and detection of infectious coxsackievirus replication using a combined cell culture-molecular beacon assay, *Appl. Environ. Microbiol.*, 2005, **71**, 8397–8401.

26 T. J. Drake, C. D. Medley, A. Sen, R. J. Rogers and W. Tan, Stochasticity of manganese superoxide dismutase mRNA expression in breast carcinoma cells by molecular beacon imaging, *ChemBioChem*, 2005, **6**, 2041–2047.

27 X. Tian, M. R. Aruva, W. Qin, W. Zhu, K. T. Duffy, E. R. Sauter, M. L. Thakur and E. Wickstrom, External imaging of CCND1 cancer gene activity in experimental human breast cancer xenografts with 99mTc-peptide-peptide nucleic acid-peptide chimeras, *J. Nucl. Med.*, 2004, **45**, 2070–2082.

28 M. R. Capecchi, High efficiency transformation by direct microinjection of DNA into cultured mammalian cells, *Cell*, 1980, **22**, 479–488.

29 E. Neumann, M. Schaefer-Ridder, Y. Wang and P. H. Hofschneider, Gene transfer into mouse lyoma cells by electroporation in high electric fields, *EMBO J.*, 1982, **1**, 841–845.

30 P. L. Felgner, T. R. Gadek, M. Holm, R. Roman, H. W. Chan, M. Wenz, J. P. Northrop, G. M. Ringold and M. Danielsen, Lipofection: a highly efficient, lipid-mediated DNA-transfection procedure, *Proc. Natl. Acad. Sci. USA*, 1987, **84**, 7413–7417.

31 L. Benimetskaya, G. B. Takle, M. Vilenchik, I. Lebedeva, P. Miller and C. A. Stein, Cationic porphyrins: novel delivery vehicles for antisense oligodeoxynucleotides, *Nucleic Acids Res.*, 1998, **26**, 5310–5317.

32 G. Cesarone, O. P. Edupuganti, C. P. Chen and E. Wickstrom, Insulin receptor substrate 1 knockdown in human MCF7 ER+ breast cancer cells by nuclease-resistant IRS1 siRNA conjugated to a disulfide-bridged D-peptide analogue of insulin-like growth factor 1, *Bioconjugate Chem.*, 2007, **18**, 1831–1840.

33 M. C. Morris, P. Vidal, L. Chaloin, F. Heitz and G. Divita, A new peptide vector for efficient delivery of oligonucleotides into mammalian cells, *Nucleic Acids Res.*, 1997, **25**, 2730–2736.

34 S. Veldhoen, S. D. Laufer, A. Trampe and T. Restle, Cellular delivery of small interfering RNA by a non-covalently attached cell-penetrating peptide: quantitative analysis of uptake and biological effect, *Nucleic Acids Res.*, 2006, **34**, 6561–6573.

35 G. M. Barton and R. Medzhitov, Retroviral delivery of small interfering RNA into primary cells, *Proc. Natl. Acad. Sci. USA*, 2002, **99**, 14943–14945.

36 R. S. Tomar, H. Matta and P. M. Chaudhary, Use of adeno-associated viral vector for delivery of small interfering RNA, *Oncogene*, 2003, **22**, 5712–5715.

37 M. J. Niedre, A. J. Secord, M. S. Patterson and B. C. Wilson, *In vitro* tests of the validity of singlet oxygen luminescence measurements as a dose metric in photodynamic therapy, *Cancer Res.*, 2003, **63**, 7986–7994.